Front. Chem. Sci. Eng. 2020, 14(1): 76–89
https://doi.org/10.1007/s11705-019-1833-0

RESEARCH ARTICLE

Diversity-oriented synthesis of blue emissive nitrogen heterocycles and their conjugation with carbon nano-onions

Viviana Maffeis[1,*], Lisa Moni[2,*], Daniele Di Stefano[2], Silvia Giordani (✉)[1,3], Renata Riva (✉)[4]

1 Nano Carbon Materials, Istituto Italiano di Tecnologia (IIT), 10144 Torino, Italy
2 Department of Chemistry and Industrial Chemistry, University of Genova, 16146 Genova, Italy
3 School of Chemical Sciences, Dublin City University, Dublin 9, Ireland
4 Department of Pharmacy, University of Genova, 16147 Genova, Italy

Abstract The search for new fluorescent molecules for possible applications as functional π-electron systems and their conjugation with different nanomaterials is nowadays of paramount importance to broaden the availability of materials with different properties. Herein we present a diversity-oriented approach to heterocyclic luminophores based on a multicomponent Ugi reaction followed by a Pd-mediated cascade sequence. The new molecules are coupled to carbon nano-onions, and hybrid systems represent the first example of blue emitters conjugated with these carbon nanoparticles.

Keywords carbon nano-onions, multicomponent reactions, blue emitters, fluorescence, isoquinolines

1 Introduction

Since the discovery of fullerene C_{60} in 1985 by Kroto, Curl and Smalley using laser desorption experiments [1], several other carbon nanomaterials were discovered in the following years. Multilayers fullerenes, also known as carbon nano-onions (CNOs), were first produced *in situ* by Ugarte in 1992 via direct irradiation of carbon soot particles by an intense electron-beam irradiation [2]. The CNOs structure consists of a hollow spherical fullerene core surrounded by carbon concentric layers with increasing diameter. The distance between the carbon layers was determined to be about 0.34 nm, which corresponds to the distance between two graphitic planes [3].

Received November 30, 2018; accepted February 8, 2019

E-mails: silvia.giordani@dcu.ie (Giordani S),
renata.riva@unige.it (Riva R)

*These authors contributed equally to this work.

After the discovery of CNOs, many efforts have been focused on the synthetic pathways to obtain these concentric spherical shell structures with higher yield and to understand the formation mechanism of such materials, as well summarized in a recent review [4]. The chemico-physical properties of CNOs are strictly dependent on the fabrication method; different synthetic protocols lead to nanoparticles of different size, shape and curvature, which ultimately translate into different chemical reactivity [5]. Over the last years, different methods of CNOs synthesis have been developed including high-temperature annealing of nanodiamonds [6], arc discharge [7,8], laser ablation [9] and chemical vapor deposition [10]. These synthetic methods affect the structure of the CNOs, the number of graphene layers and the distance between them, defining the physicochemical properties of CNOs.

In order to use CNOs in many applications, several approaches for their modification have been developed. Physical methods can be used to dope the carbon nanoparticles with metals and/or heteroatoms and chemical functionalization, either non-covalent or covalent, can impart new functionalities while improving the solubility of CNOs [11]. Actually, the pristine CNOs (*p*-CNOs) synthesized by the currently known methods are completely insoluble in all protic and aprotic solvents, because of aggregation of the nanoparticles. The first chemical functionalization of CNOs, namely an azomethine ylide addition reaction, was reported by Georgakilas et al. in 2003 [12]. Since then, many functionalization protocols have been developed [4,13–17]. The exclusive properties of CNOs, due to their unique 0-D structure compared to 1-D carbon nanotubes and 2-D graphene, high surface area/volume ratio, electrical and thermal conductivity, optical properties and excellent mechanical strength render them ideal for the future rational design of devices based on carbon nanomaterials [18–21]. Functionalized CNOs

have being proposed for a broad range of applications such as reinforcements of polymers [22,23], sensing and catalysis [24,25], solar energy conversion and storage [26,27]. Moreover, CNOs display efficient uptake and good biocompatibility [28,29] which makes these nanoparticles quite promising for biomedical applications [30,31].

Of particular relevance is the conjugation of CNOs with fluorescent molecules, because they are gaining an increasing interest as functional π-electron systems [32]. The emission of fluorescent labelled CNOs is largely dependent on the chemical and photophysical nature of the implemented fluorophores. In 2017, Prato described a bottom-up synthesis of carbon nanodots (CNDs) with tunable emission by an appropriate choice and ratio of organic chromophores [33]. This approach allowed CNDs to emit light across the entire visible spectrum, resulting in white-light emission. However, only commercially available organic building blocks, based on the naphthalene dianhydride and dibromonaphthalene dianhydride as dopants, were used. Recently, in our group, different green and red fluorophores were synthesized in order to obtain green and red emitting CNOs [34–36]. However, rationally designed CNOs as pure blue emitting materials have never been reported so far, though one example of blue emitting graphene quantum dots synthesized from CNOs has been described [37]. Therefore, we planned to synthesize a family of blue emitting CNOs, in order to complete the availability of fluorophores emitting across the entire visible spectrum. Blue emitters, in particular, are very important in the organic light emitting diode (OLED) technology [38–42]. However, their application on devices is limited by their low luminescence efficiency in aggregate state or in thin film due to aggregation caused quenching and a general low thermo-, mechano- and photostability. Common strategies to alleviate the concentration quenching, to enhance stability and to modulate optical properties, are introducing opportune bulky groups onto the fluorophore structure or conjugating the dye on suitable polymers, dendrimers or nanostructures as polyhedral oligomeric silsesquioxanes (POSS) [43]. Moreover, blue emitters-functionalized nanomaterials can find interesting applications in biophysical analytics [44], including probes of biochemistry at plasma membrane [45] and of G-quadruplex formation [46].

For our purposes, we designed and synthesized three new fluorophores to be conjugated with CNOs. These molecules are characterized by the same scaffold, a novel tricyclic furo[2,3-*c*]isoquinoline core, that was synthesized in two steps through an Ugi multicomponent reaction followed by a Pd-mediated double cyclization where an additional eight carbon fragment is incorporated. The difference between the fluorophores lies on the nature of the linker (length and polarity). They all display a primary amino group, used for the amidation of carboxylic acid groups on the CNOs surface nm. After the characterization of the new nanomaterials we demonstrated that a precise control over the structure and the energy transfer process yielding blue-CNOs has been achieved.

2 Experimental

2.1 Synthesis of furo[2,3-*c*]isoquinolines **21**–**23**

2.1.1 General

All commercially available chemicals were used without further purification unless otherwise stated. Nuclear Magnetic Resonance (NMR) spectra were taken at room temperature in $CDCl_3$ at 300 MHz (^1H) and 75 MHz (^{13}C), or 600 MHz (^1H) and 150 MHz (^{13}C) by using trimethylsilane as internal standard for ^1H NMR spectroscopy and the central peak of $CDCl_3$ (at δ 77.02 ppm) for ^{13}C NMR spectroscopy. Chemical shifts are reported in ppm (δ scale), coupling constants are reported in Hertz. Peak assignments were made with the aid of gCOSY and gHSQC, experiments. In compounds where two rotamers can be identified in the spectra *M* means the major rotamer and *m* the minor rotamer. High resolution mass spectrometry analyses were performed with a Maldi-quadrupole time-of-flight mass spectrometer equipped with Z-spray electrospray ionization source (ESI). IR spectra were recorded as solid, oil, or foamy samples, with the attenuated total reflectance technique. UV-visible absorption spectra were recorded in 3 cm (10 mm × 10 mm) cuvettes in dimethyl sulfoxide (DMSO). The wavelength range was 200−600 nm with a scan rate of 300 nm·min^{-1}. Baseline correction measurements were used for all spectra. Fluorescence measurements were made with a fluorimeter equipped with a 1.0 cm path length quartz cell. The solvents used were of HPLC grade. TLC analyses were carried out on silica gel plates and viewed at UV (λ 254 nm or 360 nm) and developed with Hanessian stain (dipping into a solution of $(NH_4)_4MoO_4\cdot 4H_2O$ (21 g) and $Ce(SO_4)_2\cdot 4H_2O$ (1 g) in H_2SO_4 (31 mL) and H_2O (469 mL) and warming) or ninhydrin. R_f values were measured after an elution of 7–9 cm. Column chromatography was done with the "flash" methodology by using 220–400 mesh silica. Petroleum ether (40°C–60°C) is abbreviated as PE. All reactions employing dry solvents were carried out under a nitrogen or an argon atmosphere.

2.1.2 General procedure for the Mitsunobu reaction (compounds **9**–**11**)

A stirred solution of *N*-(4-hydroxyphenethyl)formamide **5** (1 equiv.) in dry tetrahydrofuran (THF, 0.07 mol·L^{-1}), cooled to 0°C, was treated with the opportune alcohol (**6**, **7** or **8**, 2 equiv.), PPh_3 (2.6 equiv.) and diethyl azodicarboxylate (DEAD, 2.6 equiv.). The temperature was allowed to rise to room temperature, and the solution stirred 3 d. After

solvent evaporation the residue was eluted from a column of silica gel with the suitable eluent.

tert-Butyl(3-(4-(2-formamidoethyl)phenoxy)propyl)carbamate **9**. Compounds **5** (300 mg, 1.82 mmol) and **6** (969 mg, 5.50 mmol) were reacted as described in the general procedure. The crude was purified by column chromatography (CH_2Cl_2/PE/EtOAc/acetone 4:3:1:2) affording **9** as a white solid (464 mg, 79%). M.p. 77.1°C–78.3°C (CH_2Cl_2). R_f 0.25 (CH_2Cl_2/PE/EtOAc/acetone 4:3:1:2). ^{1}H NMR (300 MHz, $CDCl_3$, 80:20 mixture of rotamers, δ ppm): 8.14 (*M*) (s, 0.8 H, CHO), 7.93 (*m*) (d, *J* = 12.0 Hz, 0.2 H, CHO), 7.15–7.04 (*m* + *M*) (m, 2 H, CH Ar), 6.88–6.77 (*m* + *M*) (m, 2 H, CH Ar), 5.46 (*m* + *M*) (broad s, 1 H, NH), 4.75 (*m* + *M*) (broad s, 1 H, NH), 4.00 (*m* + *M*) (t, *J* = 6.0 Hz, 2 H, CH_2OAr), 3.54 (*m* + *M*) (q, *J* = 6.5 Hz, 2 H, CH_2), 3.38–3.25 (*m* + *M*) (m, 2 H, CH_2NH), 2.78 (*M*) (t, *J* = 6.9 Hz, 1.6 H, CH_2Ar), 2.75 (*m*) (t, *J* = 6.6 Hz, 0.4 H, CH_2Ar), 1.97 (*m* + *M*) (quint, *J* = 6.4 Hz, 2 H, CH_2), 1.44 (*m* + *M*) (s, 9 H, Boc). ^{13}C NMR (75 MHz, $CDCl_3$, δ ppm): 164.4 (CHO *m*), 161.1 (CHO *M*), 157.5 (C quat. *m* + *M*), 156.0 (C quat. *m* + *M*), 130.6 (C quat. *m* + *M*), 129.8 (2 CH *m*), 129.7 (2 CH *M*), 114.8 (2 CH *m*), 114.6 (2 CH *M*), 79.1 (C quat. *m* + *M*), 65.8 (CH_2m + *M*), 43.3 (CH_2m), 39.3 (CH_2M), 38.0 (CH_2m), 36.8 (CH_2M), 34.6 (CH_2m + *M*), 29.5 (CH_2m + *M*), 28.4 (Boc *m* + *M*). IR ($CHCl_3$, $\tilde{\nu}$): 3365, 3309, 2983, 2969, 2936, 2879, 1683, 1647, 1611, 1583, 1523, 1512, 1473, 1440, 1388, 1367, 1325, 1299, 1272, 1237, 1165, 1117, 1059, 1007, 944, 864, 837, 817, 803, 781, 748, 721, 696, 615 cm^{-1}. HRMS (ESI$^+$): *m/z* calcd for $C_{17}H_{27}N_2O_4$ $[M + H]^+$ 323.1971, found 323.1976.

tert-Butyl(2-(4-(2-formamidoethyl)phenoxy)ethyl)carbamate **10**. Compounds **5** (303 mg, 1.83 mmol) and **7** (0.56 mL, 3.63 mmol) were reacted as described in the general procedure. After 3 d, PPh_3 (1 equiv.), DEAD (1 equiv.) and alcohol (1.5 equiv.) were added and the mixture was stirred for additional 5 d. The crude was purified by column chromatography (CH_2Cl_2/PE/EtOAc/acetone 4:3:1:2) affording **10** as a white foam (302 mg, 53%). R_f 0.31 (CH_2Cl_2/PE/EtOAc/acetone 4:3:1:2). ^{1}H NMR (300 MHz, $CDCl_3$, 84:16 mixture of rotamers, δ ppm): 8.14 (*M*) (s, 0.8 H, CHO), 7.93 (*m*) (d, *J* = 12.0 Hz, 0.2 H, CHO), 7.16–7.05 (*m* + *M*) (m, 2 H, CH Ar), 6.90–6.78 (*m* + *M*) (m, 2 H, CH Ar), 5.50 (*m* + *M*) (broad s, 1 H, NH), 4.99 (*m* + *M*) (broad s, 1 H, NH), 4.00 (*m* + *M*) (t, *J* = 5.1 Hz, 2 H, CH_2OAr), 3.65–3.47 (*m* + *M*) (m, 4 H, 2 CH_2), 2.79 (*m* + *M*) (t, *J* = 6.9 Hz, 2 H, CH_2Ar), 1.45 (*m* + *M*) (s, 9 H, Boc). ^{13}C NMR (75 MHz, $CDCl_3$, δ ppm): 164.3 (CHO *m*), 161.1 (CHO *M*), 157.5 (C quat. *m*), 157.4 (C quat. *M*), 155.9 (C quat. *m* + *M*), 132.2 (C quat. *m*), 130.8 (C quat. *m* + *M*), 129.9 (2 CH *m*), 129.8 (2 CH *M*), 114.8 (2 CH *m*), 114.7 (2 CH *M*), 79.6 (C quat. *m* + *M*), 67.2 (CH_2m + *M*), 43.2 (CH_2m), 40.1 (CH_2M), 39.3 (CH_2m + *M*), 36.9 (CH_2m), 34.6 (CH_2M), 28.4 (Boc *m* + *M*). IR ($CHCl_3$, $\tilde{\nu}$): 3370, 3325, 2981, 2934, 2883, 2861, 1687, 1663, 1616, 1584, 1513, 1465, 1455, 1421, 1387, 1367, 1296, 1276, 1233, 1204, 1188, 1159, 1113, 1060, 1041, 1035, 1011, 982, 931, 894, 862, 826, 815, 802, 783, 772, 762, 720, 708, 612 cm^{-1}. HRMS (ESI$^+$): *m/z* calcd for $C_{16}H_{25}N_2O_4$ $[M + H]^+$ 309.1814, found 309.1819.

tert-Butyl(2-(2-(4-(2-formamidoethyl)phenoxy)ethoxy)ethyl)carbamate **11**. Phenol **5** (297 mg, 1.80 mmol) **8** (734 mg, 3.58 mmol) were reacted as described in the general procedure. PPh_3 (1 equiv.), DEAD (1 equiv.) and alcohol (1 equiv.) were added to the reaction mixture after 3 and 2 d respectively and finally the mixture was stirred for additional 2 d. The crude was purified by column chromatography (CH_2Cl_2/PE/EtOAc/acetone 4:3:1:2). The obtained residue resulted still contaminated by unreacted phenol **5**; therefore it was diluted with CH_2Cl_2 (20 mL) and washed with Na_2CO_3 (10 mL × 5), affording **11** as a white solid (394 mg, 62%). M. p. 62.0°C–62.7°C (CH_2Cl_2). R_f 0.24 (CH_2Cl_2/PE/EtOAc/acetone 4:3:1:2). ^{1}H NMR (300 MHz, $CDCl_3$, 85:15 mixture of rotamers, δ ppm): 8.13 (*M*) (d, *J* = 1.3 Hz, 0.8 H, CHO), 7.92 (*m*) (d, *J* = 12.0 Hz, 0.2 H, CHO), 7.17–7.04 (*m* + *M*) (m, 2 H, CH Ar), 6.94–6.84 (*m* + *M*) (m, 2 H, CH Ar), 5.52 (*m* + *M*) (broad s, 1 H, NH), 4.96 (*m* + *M*) (broad s, 1 H, NH), 4.13–4.06 (*m* + *M*) (m, 2 H, CH_2), 3.86–3.77 (*m* + *M*) (m, 2 H, CH_2), 3.63–3.57 (*m* + *M*) (m, 2 H, CH_2), 3.57–3.50 (*m* + *M*) (m, 2 H, CH_2), 3.37–3.27 (*m* + *M*) (m, 2 H, CH_2), 2.78 (*M*) (t, *J* = 6.9 Hz, 1.6 H, CH_2), 2.75 (*m*) (t, *J* = 6.8 Hz, 0.4 H, CH_2), 1.44 (*m* + *M*) (s, 9 H, Boc). ^{13}C NMR (75 MHz, $CDCl_3$, δ ppm): 164.4 (C quat. *m*), 161.2 (C quat. *M*), 157.1 (C quat. *m*), 157.0 (C quat. *M*), 155.7 (C quat. *m* + *M*), 130.7 (C quat. *m* + *M*), 129.5 (2 CH Ar *m*)129.3 (2 CH Ar *M*), 114.5 (2 CH Ar *m*), 114.3 (2 CH Ar *M*), 78.7 (C quat. *m* + *M*), 69.9 (CH_2m + *M*), 69.0 (CH_2m + *M*), 66.9 (CH_2m + *M*), 39.9 (CH_2m + *M*), 39.1 (CH_2m + *M*), 36.4 (CH_2m), 34.2 (CH_2M), 28.9 (Boc *m*), 28.0 (Boc *M*). IR ($CHCl_3$, $\tilde{\nu}$): 3339, 2975, 2957, 2928, 2886, 1700, 1676, 1528, 1513, 1453, 1383, 1364, 1327, 1302, 1279, 1242, 1180, 1125, 1079, 1058, 969, 923, 895, 876, 834, 812, 785, 767, 731, 714, 631, 604 cm^{-1}. HRMS (ESI$^+$): *m/z* calcd for $C_{18}H_{29}N_2O_5$ $[M + H]^+$ 353.2076, found 353.2081.

2.1.3 General procedure for the isocyanide formation (compounds **12**–**14**)

A solution of formamide (**9**, **10** or **11**, 0.60–0.90 mmol, 1 equiv.) in dry CH_2Cl_2 (0.22 mol·L^{-1}) was cooled to –30°C. Triethylamine (7.5 equiv.) and $POCl_3$ (3.4 equiv.) were successively added, keeping the temperature not higher than –30°C. After 3 h, the mixture was quenched with a saturated aqueous solution of $NaHCO_3$ (30 mL), extracted with CH_2Cl_2 (3 × 10 mL). Then the organic phases were washed with brine (20 mL), dried (Na_2SO_4), and concentrated.

tert-Butyl(3-(4-(2-isocyanoethyl)phenoxy)propyl)carbamate **12**. Formamide **9** (343 mg, 0.93 mmol) was

dehydrated as described in the general procedure. The crude was eluted from a column of silica gel with PE/EtOAc (1:3) to give **12** (165 mg, 58%) as a white foam. R_f 0.30 (PE/EtOAc 1:3). ^{1}H NMR ($CDCl_3$, 300 MHz, δ ppm): 7.17–7.09 (m, 2 H, CH Ar), 6.89–6.83 (m, 2 H, CH Ar), 4.78 (broad s, 1 H, NH), 4.00 (t, J = 6.0 Hz, 2 H, CH_2), 3.56 (t, J = 6.9 Hz, 2 H, CH_2), 3.31 (q, J = 6.3 Hz, 2 H, CH_2), 2.92 (t, J = 6.9 Hz, 2 H, CH_2), 1.97 (quint, J = 6.3 Hz, 2 H, CH_2), 1.44 (s, 9 H, Boc). ^{13}C NMR (75 MHz, $CDCl_3$, δ ppm): 157.9 (C = O), 156.3 (C quat.), 156.0 (C quat.), 129.7 (2 CH Ar), 128.8 (C quat.), 114.7 (2 CH Ar), 79.2 (C quat.), 65.8 (CH_2), 43.2 (CH_2), 38.0 (CH_2), 34.8 (CH_2), 29.5 (CH_2), 28.4 (Boc). IR ($CHCl_3$, $\tilde{\nu}$): 3357, 2980, 2933, 2145, 1698, 1615, 1579, 1511, 1457, 1392, 1360, 1243, 1165, 1123, 1064, 1044, 977, 910, 861, 833, 805, 781, 730, 647 cm^{-1} HRMS (ESI$^+$): *m/z* calcd for $C_{17}H_{25}N_2O_3$ $[M + H]^+$ 305.1856, found 305.1862.

tert-Butyl(2-(4-(2-isocyanoethyl)phenoxy)ethyl)carbamate **13**. Formamide **10** (268 mg, 0.77 mmol) was dehydrated as described in the general procedure. The crude was eluted from a column of silica gel with PE/Et_2O (1:1) to give **13** (147 mg, 66%) as a colorless oil. R_f 0.27 (PE/Et_2O 1:1). ^{1}H NMR ($CDCl_3$, 300 MHz, δ ppm): 7.18–7.11 (m, 2 H, CH Ar), 6.89–6.83 (m, 2 H, CH Ar), 4.98 (broad s, 1 H, NH), 4.01 (t, J = 5.1 Hz, 2 H, CH_2), 3.62–3.48 (m, 4 H, 2 CH_2), 2.93 (t, J = 7.0 Hz, 2 H, CH_2), 1.45 (s, 9 H, Boc). ^{13}C NMR (75 MHz, $CDCl_3$, δ ppm): 157.9 (C = O), 156.5 (C quat.), 156.0 (C quat.), 129.9 (2 CH Ar), 129.2 (C quat.), 114.8 (2 CH Ar), 79.7 (C quat.), 67.3 (CH_2), 43.3 (CH_2), 40.2 (CH_2), 34.9 (CH_2), 28.5 (Boc). IR ($CHCl_3$, $\tilde{\nu}$): 3357, 2977, 2933, 2147, 1697, 1612, 1584, 1511, 1457, 1392, 1366, 1243, 1165, 1113, 1064, 1041, 977, 910, 861, 833, 805, 781, 730, 647 cm^{-1}. HRMS (ESI$^+$): *m/z* calcd for $C_{16}H_{23}N_2O_3$ $[M + H]^+$ 291.1709, found 291.1703.

tert-Butyl(2-(2-(4-(2-isocyanoethyl)phenoxy)ethoxy) ethyl)carbamate **14**. Formamide **11** (240 mg, 0.61 mmol) was dehydrated as described in the general procedure. The crude was eluted from a column of silica gel with PE/EtOAc (2:1) to give **14** (160 mg, 70%) as white solid. M.p. 70.9°C–71.5°C (CH_2Cl_2). R_f 0.31 (PE/EtOAc 2:1). ^{1}H NMR ($CDCl_3$, 300 MHz) δ 7.17–7.11 (m, 2 H, 2 CH Ar), 6.93–6.86 (m, 2 H, 2 CH Ar), 4.97 (broad s, 1 H, NH), 4.11 (dd, J = 5.5, 4.0 Hz, 2 H, CH_2), 3.82 (dd, J = 5.4, 4.0 Hz, 2 H, CH_2), 3.66–3.52 (m, 4 H, 2 CH_2), 3.34 (q, J = 5.3 Hz, 2 H, CH_2), 2.93 (t, J = 7.1 Hz, 2 H, CH_2), 1.44 (s, 9 H, Boc). ^{13}C NMR (75 MHz, $CDCl_3$, δ ppm): 157.9 (C quat.), 156.3 (C quat.), 155.9 (C quat.), 129.7 (2 CH Ar), 129.0 (C quat.), 114.8 (2 CH Ar), 79.2 (C quat.), 70.4 (CH_2), 69.4 (CH_2), 67.3 (CH_2), 43.2 (CH_2), 40.3 (CH_2), 34.8 (CH_2), 28.4 (Boc). IR ($CHCl_3$, $\tilde{\nu}$): 3335, 2972, 2928, 2888, 2872, 2158, 1698, 1676, 1610, 1582, 1530, 1514, 1453, 1382, 1364, 1328, 1302, 1281, 1243, 1168, 1126, 1079, 1058, 1032, 970, 949, 923, 897, 876, 832, 814, 798, 768, 714, 637, 605 cm^{-1}. HRMS (ESI$^+$): *m/z* calcd for $C_{18}H_{27}N_2O_4$ $[M + H]^+$ 335.1971, found 335.1976.

2.1.4 General procedure for the Ugi reaction (compounds **15**–**17**)

A stirred solution of 2-iodobenzaldehyde (1 equiv.) in CF_3CH_2OH/EtOH (1:1, 0.35 mol·L^{-1}) containing molecular sieves (4 Å, 25 mg·mmol^{-1} aldehyde), was treated at room temperature with 2,4-dimethoxybenzylamine (1.05 equiv.). After 1 h the solution was treated at room temperature with phenylpropiolic acid (1.05 equiv.) and the isocyanide (**12**, **13** or **14**, 1.05 equiv.). The mixture was stirred for 24–48 h, then filtered through a celite cake, washed with CH_2Cl_2, and concentrated. The crude was eluted from a column of silica gel with the suitable eluent.

tert-Butyl(3-(4-(2-(2-(*N*-(2,4-dimethoxybenzyl)-3-phenylpropiolamido)-2-(2-iodophenyl)acetamido) ethyl)phenoxy)propyl)carbamate **15**. The Ugi reaction, starting from 2-iodobenzaldehyde (115 mg, 0.49 mmol), 2,4-dimethoxybenzylamine (83 μL, 0.52 mmol), phenylpropiolic acid (77 mg, 0.52 mmol) and isocyanide **12** (160 mg, 0.52 mmol), was carried out as described in the general procedure. The crude was purified by column chromatography (CH_2Cl_2/PE/EtOAc 2:3:2) affording **15** as a white foam (356 mg, 87%). R_f 0.34 (PE/CH_2Cl_2/EtOAc 3:2:2). ^{1}H NMR ($CDCl_3$, 300 MHz, δ ppm, 75:15 mixture of rotamers): 7.79 (*m*) (dd, J = 8.1, 1.3 Hz, 0.15 H, CH Ar), 7.71 (*M*) (dd, J = 7.9, 1.2 Hz, 0.75 H, CH Ar), 7.62–7.54 (*m*) (m, 0.3 H, CH Ar), 7.53–7.46 (*M*) (m, 1.7 H, CH Ar), 7.45–7.28 (*M* + *m*) (m, 4 H, CH Ar), 7.20 (*M* + *m*) (td, J = 7.8, 4.2 Hz, 1 H, CH Ar), 7.14–6.85 (*M* + *m*) (m, 5 H, CH Ar and NH), 6.83–6.69 (*M* + *m*) (m, 2 H, CH Ar), 6.32 (*M*) (dd, J = 8.4, 2.4 Hz, 0.75 H, CH Ar), 6.30 (*m*) (dd, J = 7.7, 2.5 Hz, 0.15 H, CH Ar), 6.25 (*m*) (d, J = 2.4 Hz, 1 H, CH Ar), 6.22 (*M*) (d, J = 2.4 Hz, 1 H, CH Ar), 5.76 (*M*) (t, J = 5.9 Hz, 0.75 H, NH), 5.61 (*M* + *m*) (s, 1 H, CH), 4.98 and 4.68 (*M*) (AB syst., J = 15.9 Hz, 1.7 H, NCH_2Ar), 4.74 (*M* + *m*) (broad s, 1 H, NH), 4.74 and 3.96 (*m*) (AB syst., J = 16.3 Hz, 0.3 H, NCH_2Ar), 3.94 (*M* + *m*) (t, J = 6.0 Hz, 2 H, CH_2), 3.76 (*m*) (s, 0.45 H, OMe), 3.75 (*M*) (s, 2.25 H, OMe), 3.63 (*M*) (s, 2.25 H, OMe), 3.61 (*m*) (s, 0.45 H, OMe), 3.57–3.40 (*M* + *m*) (m, 1 H, CH_2), 3.40–3.22 (*M* + *m*) (m, 3 H, CH_2), 2.67 (*M*) (t, J = 6.9 Hz, 1.7 H, CH_2), 2.62–2.51 (*m*) (m, 0.3 H, CH_2), 1.97–1.88 (*M* + *m*) (m, 2 H, CH_2), 1.44 (*M* + *m*) (s, 9 H, Boc). ^{13}C NMR (75 MHz, $CDCl_3$, δ ppm, only major rotamer is reported): 167.8 (C = O), 160.6 (C = O), 158.0 (C quat.), 157.3 (C quat.), 156.0 (C quat.), 155.9 (C quat.), 139.5 (CH Ar), 137.0 (C quat.), 132.4 (2 CH Ar), 131.3 (CH Ar), 130.8 (CH Ar), 130.6 (CH Ar), 130.0 (CH Ar), 129.8 (2 CH Ar), 129.6 (C quat.), 128.5 (2 CH Ar), 128.1 (CH Ar), 120.5 (C quat.), 116.4 (C quat.), 114.5 (2 CH Ar), 103.9 (CH Ar), 102.5 (C quat.), 98.1 (CH Ar), 90.8 (C quat.), 82.1 (C quat.), 79.2 (C quat.), 68.2 (CH), 65.8 (CH_2), 55.4 (OCH_3), 55.0 (OCH_3), 47.9 (CH_2), 41.2 (CH_2), 38.1 (CH_2), 34.6 (CH_2), 29.5 (CH_2), 28.4 (Boc). IR ($CHCl_3$, $\tilde{\nu}$): 3323, 2970, 2932, 2215, 1678, 1612, 1589, 1508, 1461, 1403, 1365, 1243, 1207, 1158, 1121, 1031, 920, 821, 757, 690, 638 cm^{-1}. HRMS (ESI$^+$):

m/z calcd for $C_{42}H_{46}IN_3NaO_7$ $[M + Na]^+$ 854.2278, found 854.2273.

tert-Butyl(2-(4-(2-(2-(*N*-(2,4-dimethoxybenzyl)-3-phenylpropiolamido)-2-(2-iodophenyl)acetamido) ethyl)phenoxy)ethyl)carbamate **16**. The Ugi reaction, starting from 2-iodobenzaldehyde (112 mg, 0.48 mmol), 2,4-dimethoxybenzylamine (81 μL, 0.51 mmol), phenylpropiolic acid (74 mg, 0.51 mmol) and isocyanide **13** (147 mg, 0.51 mmol), was carried out as described in the general procedure. The crude was purified by column chromatography (CH_2Cl_2/PE/EtOAc 2:3:2) affording **16** as a white foam (319 mg, 81%). R_f 0.35 (PE/CH_2Cl_2/EtOAC 3:2:2). ^{1}H NMR ($CDCl_3$, 300 MHz, δ ppm, 78:22 mixture of rotamers): 7.79 (*m*) (dd, *J* = 7.8, 1.0 Hz, 0.2 H, CH Ar), 7.71 (*M*) (dd, *J* = 7.9, 1.1 Hz, 0.8 H, CH Ar), 7.61–7.53 (*m*) (m, 0.4 H, CH Ar), 7.53–7.45 (*M*) (m, 1.6 H, CH Ar), 7.45–7.31 (*M* + *m*) (m, 4 H, CH Ar), 7.21 (*M* + *m*) (t, *J* = 7.7 Hz, 1 H; CH Ar), 7.14–6.89 (*M* + *m*) (m, 5 H, CH Ar and NH), 6.81–6.67 (*M* + *m*) (m, 2 H, CH Ar), 6.33 (*M*) (dd, *J* = 8.4, 2.3 Hz, 0.8 H; CH Ar), 6.30 (*m*) (dd, *J* = 6.7, 2.3 Hz, 0.2 H, CH Ar), 6.24 (*m*) (d, *J* = 2.4 Hz, 0.2 H, CH Ar), 6.22 (*M*) (d, *J* = 2.3 Hz, 0.8 H, CH Ar), 5.79 (*M*) (t, *J* = 5.7 Hz, 0.8 H, NH), 5.61 (*M* + *m*) (s, 1 H, CH), 4.98 (*m*) (broad s, 0.2 H, NH), 4.98 and 4.69 (*M*) (AB syst., *J* = 15.8 Hz, 1.6 H, NCH_2Ar), 4.74 and 4.13 (*m*) (AB syst., *J* = 15.3 Hz, 0.4 H, NCH_2Ar), 4.00–3.89 (*M* + *m*) (m, 2 H, CH_2), 3.76 (*m*) (s, 0.6 H, OMe), 3.75 (*M*) (s, 2.4 H, OMe), 3.63 (*m*) (s, 0.6 H, OMe), 3.61 (*M*) (s, 2.4 H, OMe), 3.58–3.41 (*M* + *m*) (m, 3 H, CH_2), 3.41–3.23 (*M* + *m*) (m, 1 H, CH_2), 2.67 (*M*) (t, *J* = 6.9 Hz, 1.6 H, CH_2), 2.63–2.52 (*m*) (m, 0.4 H, CH_2), 1.45 (*M* + *m*) (s, 9 H, Boc). ^{13}C NMR (75 MHz, $CDCl_3$, δ ppm, only major rotamer is reported): 167.8 (C = O), 160.6 (C = O), 158.0 (C quat.), 157.1 (C quat.), 156.0 (C quat.), 155.8 (C quat.), 139.6 (CH Ar), 137.1 (C quat.), 132.4 (2 CH Ar), 131.4 (CH Ar), 130.8 (CH Ar), 130.6 (CH Ar), 130.1 (CH Ar), 129.9 (2 CH Ar), 129.7 (C quat.), 128.5 (2 CH Ar), 128.1 (CH Ar), 120.5 (C quat.), 116.4 (C quat.), 114.5 (2 CH Ar), 103.9 (CH Ar), 102.5 (C quat.), 98.1 (CH Ar), 90.8 (C quat.), 82.1 (C quat.), 79.2 (C quat.), 68.3 (CH), 67.1 (CH_2), 55.4 (OCH_3), 55.0 (OCH_3), 47.9 (CH_2), 41.2 (CH_2), 40.1 (CH_2), 34.6 (CH_2), 28.4 (Boc). IR ($CHCl_3$, $\tilde{\nu}$): 3323, 2970, 2932, 2215, 1678, 1612, 1589, 1508, 1461, 1403, 1365, 1243, 1207, 1158, 1121, 1031, 920, 821, 757, 690, 638 cm^{-1}. HRMS (ESI^+): *m/z* calcd for $C_{41}H_{44}IN_3NaO_7$ $[M + Na]^+$ 840. 2122, found 840.2116.

tert-Butyl(2-(2-(4-(2-(2-(*N*-(2,4-dimethoxybenzyl)-3-phenylpropiolamido)-2-(2-iodophenyl) acetamido)ethyl) phenoxy)ethoxy)ethyl)carbamate **17**. The Ugi reaction, starting from 2-iodobenzaldehyde (134 mg, 0.58 mmol), 2,4-dimethoxybenzylamine (97 μL, 0.61 mmol), phenylpropiolic acid (88 mg, 0.61 mmol) and isocyanide **14** (185 mg, 0.52 mmol), was carried out as described in the general procedure, except for the temperature (the reaction mixture was stirred at 45°C). The crude was purified by column chromatography (CH_2Cl_2/EtOAc 5:1 + MeOH 1%) affording **17** as a white foam (376 mg, 79%). R_f 0.29 (CH_2Cl_2/EtOAc 5:1 + MeOH 1%). ^{1}H NMR ($CDCl_3$, 300 MHz) (68:32 mixture of rotamers): δ 7.79 (*m*) (d, *J* = 8.0 Hz, 0.3 H, CH Ar), 7.71 (*M*) (dd, *J* = 7.9, 1.1 Hz, 0.7 H, CH Ar), 7.62–7.55 (*m*) (m, 0.6 H, CH Ar), 7.53–7.46 (*M*) (m, 1.4 H, CH Ar), 7.45–7.30 (*M* + *m*) (m, 3 H, CH Ar), 7.26–7.16 (*M* + *m*) (m, 1 H, CH Ar), 7.14–6.86 (*M* + *m*) (m, 5.3 H, CH Ar and NH), 6.84–6.75 (*M* + *m*) (m, 2 H, CH Ar), 6.33 (*M*) (dd, *J* = 8.4, 2.3 Hz, 0.7 H, CH Ar), 6.30–6.28 (*m*) (m, 0.3 H, CH Ar), 6.25 (*m*) (d, *J* = 2.3 Hz, 0.3 H, CH Ar), 6.22 (*M*) (d, *J* = 2.3 Hz, 0.7 H, CH Ar), 6.20 (*M*) (broad s, 0.7 H, NH), 5.78 (*M*) (t, *J* = 5.5 Hz, 0.7 H, NH), 5.62 (*M* + *m*) (s, 1 H, CH), 4.99 (*m*) (m, 0.3 H, NH), 4.98 and 4.69 (*M*) (AB syst., *J* = 15.8 Hz, 1.4 H, NCH_2Ar), 4.74 and 4.12 (*m*) (AB syst., *J* = 16.5 Hz, 0.6 H, NCH_2Ar), 4.09–3.95 (*M* + *m*) (m, 2 H, CH_2), 3.87–3.68 (*M* + *m*) (m, 5 H, CH_2 and OMe), 3.63–3.57 (*M* + *m*) (m, 5 H, CH_2 and OMe), 3.51–3.42 (*M* + *m*) (m, 2 H, CH_2), 3.41–3.18 (*M* + *m*) (m, 2 H, CH_2), 2.67 (*M*) (t, *J* = 6.9 Hz, 1.4 H, CH_2), 2.63–2.50 (*m*) (m, 0.6 H, CH_2), 1.44 (*M* + *m*) (s, 9 H, Boc). ^{13}C NMR (75 MHz, $CDCl_3$, δ ppm, mixture of rotamers): 168.8 (C = O *m*), 167.8 (C = O *M*), 160.5 (C = O *M*), 160.3 (C = O *m*), 158.0 (C quat. *M*), 157.4 (C quat. *m*), 157.3 (C quat. *m*), 157.2 (2 C quat. *M*), 156.9 (C quat. *m*), 156.0 (C quat. *M*), 155.9 (C quat. *m*), 139.7 (CH Ar *m*), 139.5 (CH Ar *M*), 137.0 (C quat. *M*), 136.6 (C quat. *m*), 132.8 (2 CH Ar *m*), 132.4 (2 CH Ar *M*), 131.3 (CH Ar *M*), 131.2 (CH Ar *m*), 130.8 (CH Ar *M*), 130.7 (CH Ar *m*), 130.6 (CH Ar *M*), 130.4 (CH Ar *m*), 130.0 (CH Ar *M*), 130.0 (CH Ar *m*), 129.8 (2 CH Ar *M* + *m*), 129.6 (C quat. *M* + *m*), 128.5 (2 CH Ar *m*), 128.5 (2 CH Ar *M*), 128.1 (CH Ar *M*), 127.8 (CH Ar *m*), 120.5 (C quat. *M*), 120.1 (C quat. *m*), 117.2 (C quat. *m*), 116.4 (C quat. *M*), 114.7 (2 CH Ar *m*), 114.6 (2 CH Ar *M*), 104.2 (CH Ar *m*), 103.9 (CH Ar *M*), 103.0 (C quat. *m*), 102.5 (C quat. *M*), 98.1 (CH Ar *m*), 98.0 (CH Ar *M*), 92.2 (C quat. *m*), 90.7 (C quat. *M*), 82.1 (C quat. *M*), 81.9 (C quat. *m*), 79.2 (C quat. *M* + *m*), 71.5 (CH *m*), 70.3 ($CH_2M + m$), 69.4 ($CH_2M + m$), 68.2 (CH *M*), 67.3 ($CH_2M + m$), 55.3 ($OCH_3M + m$), 55.1 (OCH_3m), 55.0 (OCH_3M), 47.8 (CH_2M + *m*), 41.2 (CH_2M), 41.1 (CH_2m), 40.9 (CH_2m), 40.3 (CH_2M), 34.7 (CH_2m), 34.6 (CH_2M), 28.4 (Boc *M* + *m*). IR ($CHCl_3$, $\tilde{\nu}$): 3323, 2971, 2930, 2872, 2215, 1680, 1613, 1589, 1508, 1453, 1404, 1365, 1245, 1207, 1158, 1121, 1033, 1014, 920, 823, 757, 731, 690, 638 cm^{-1}. HRMS (ESI^+): *m/z* calcd for $C_{43}H_{48}IN_3NaO_8$ $[M + Na]^+$ 884.2384, found 884.2378.

2.1.5 General procedure for the synthesis of furo[2,3-*c*] isoquinolines (compounds **18**–**20**)

A solution of the Ugi product (**15**, **16** or **17**) in MeCN/Et_3N (1:1, 0.1 mol·L^{-1}) under an argon atmosphere, was treated with $PdCl_2(PPh_3)_2$ (0.05 equiv.) and the opportune alkyne (2 equiv.) at 90°C with microwave heating for 1 h. After

this time, 1,5-diazabicyclo(5.4.0)undec-7-ene (DBU, 1 equiv.) was added and the mixture was stirred at 110°C under microwave heating for 1 h. Then, the crude was diluted with CH_2Cl_2, washed with saturated aqueous NH_4Cl, dried (Na_2SO_4), and concentrated. The residue was eluted from a column of silica gel with the suitable eluent.

tert-Butyl (3-(4-(2-(2-benzyl-1-phenylfuro[2,3-c]isoquinoline-5-carboxamido)ethyl)phenoxy)propyl) carbamate **18**. The reaction between **15** (83 mg, 0.10 mmol), $PdCl_2(PPh_3)_2$ (3.5 mg, 5.10 μmol), phenylacetylene (22 μL, 0.20 mmol) and DBU (15 μL, 0.10 mmol) was carried out as described in the general procedure. The crude was eluted from a column of silica gel with PE/CH_2Cl_2/EtOAc (4:2:1) to give **18** (43 mg, 66%) as a yellow foam. R_f 0.32 (PE/CH_2Cl_2/EtOAc 4:2:1). ^{1}H NMR ($CDCl_3$, 300 MHz, δ ppm): 9.72 (dd, J = 7.8, 1.2 Hz, 1 H, CH Ar), 8.13 (broad t, J = 6.0 Hz, 1 H, NH), 7.77 (dd, J = 7.4, 1.5 Hz, 1 H, CH Ar), 7.61–7.45 (m, 7 H, 7 CH Ar), 7.38–7.16 (m, 7 H, 7 CH Ar), 6.84 (broad d, J = 8.6 Hz, 2 H, 2 CH Ar), 4.78 (broad s, 1 H, NH), 4.13 (s, 2 H, CH_2), 4.00 (t, J = 6.0 Hz, 2 H, CH_2), 3.74 (q, J = 6.7 Hz, 2 H, CH_2), 3.32 (q, J = 6.1 Hz, 2 H, CH_2), 2.94 (t, J = 7.3 Hz, 2 H, CH_2), 2.09–1.85 (m, 2 H, CH_2), 1.44 (s, 9 H, Boc). ^{13}C NMR (75 MHz, $CDCl_3$, δ ppm): 166.0 (C quat.), 157.4 (C quat.), 156.0 (C quat.), 154.5 (C quat.), 154.4 (C quat.), 142.6 (C quat.), 137.2 (C quat.), 133.0 (C quat.), 132.3 (C quat.), 131.3 (C quat.), 130.3 (2 CH Ar), 130.0 (CH Ar), 129.8 (2 CH Ar), 129.1 (CH Ar), 129.0 (2 CH Ar), 128.7 (2 CH Ar), 128.6 (2 CH Ar), 128.4 (CH Ar), 126.8 (CH Ar), 126.3 (CH Ar), 125.2 (C quat.), 122.5 (CH Ar), 119.5 (C quat.), 116.3 (C quat.), 114.6 (2 CH Ar), 79.2 (C quat.), 65.8 (CH_2), 41.3 (CH_2), 38.1 (CH_2), 35.1 (CH_2), 32.8 (CH_2), 29.5 (CH_2), 28.4 (Boc). IR ($CHCl_3$, $\tilde{\nu}$): 3359, 2967, 2929, 2872, 1677, 1650, 1618, 1567, 1513, 1441, 1384, 1365, 1330, 1242, 1165, 1109, 1029, 1013, 981, 889, 864, 807, 786, 768, 753, 704, 651 cm^{-1}. HRMS (ESI$^+$): *m/z* calcd for $C_{41}H_{41}N_3NaO_5$ $[M + Na]^+$ 678.2944, found 678.2938.

tert-Butyl(2-(4-(2-(2-benzyl-1-phenylfuro[2,3-c]isoquinoline-5-carboxamido)ethyl)phenoxy) ethyl)carbamate **19**. The reaction between **16** (115 mg, 0.14 mmol), $PdCl_2(PPh_3)_2$ (5.0 mg, 7.10 μmol), phenylacetylene (31 μL, 0.28 mmol) and DBU (21 μL, 0.14 mmol) was carried out as described in the general procedure. The crude was eluted from a column of silica gel with PE/CH_2Cl_2/EtOAc (4:2:1) to give **19** (90 mg, 84%) as a yellow oil. R_f 0.34 (PE/CH_2Cl_2/EtOAc 4:2:1). ^{1}H NMR ($CDCl_3$, 300 MHz, δ ppm): 9.72 (dd, J = 7.9, 1.2 Hz, 1 H, CH Ar), 8.13 (broad t, J = 6.0 Hz, 1 H, NH), 7.77 (dd, J = 7.5, 1.3 Hz, 1 H, CH Ar), 7.61–7.44 (m, 7 H, 7 CH Ar), 7.34–7.15 (m, 7 H, 7 CH Ar), 6.89–6.79 (m, 2 H, 2 CH Ar), 5.00 (broad s, 1 H, NH), 4.13 (s, 2 H, CH_2), 3.99 (t, J = 5.1 Hz, 2 H, CH_2), 3.74 (dt, J = 7.3, 6.5 Hz, 2 H, CH_2), 3.56–3.45 (m, 2 H, CH_2), 2.94 (t, J = 7.3 Hz, 2 H, CH_2), 1.45 (s, 9 H, Boc). ^{13}C NMR (75 MHz, $CDCl_3$, δ ppm): 166.0 (C quat.), 157.2 (C quat.), 155.9 (C quat.), 154.5 (2 C quat.), 142.6 (C quat.), 137.2 (C quat.), 133.0 (C quat.), 132.3 (C quat.), 131.6 (C quat.), 130.4 (2 CH Ar), 130.0 (CH Ar), 129.9 (2 CH Ar), 129.1 (CH Ar), 129.0 (2 CH Ar), 128.7 (2 CH Ar), 128.6 (2 CH Ar), 128.4 (CH Ar), 126.8 (CH Ar), 126.3 (CH Ar), 125.2 (C quat.), 122.5 (CH Ar), 119.6 (C quat.), 116.3 (C quat.), 114.6 (2 CH Ar), 79.2 (C quat.), 67.2 (CH_2), 41.3 (CH_2), 40.2 (CH_2), 35.1 (CH_2), 32.8 (CH_2), 28.4 (Boc). IR ($CHCl_3$, $\tilde{\nu}$): 3332, 2970, 2930, 2872, 1707, 1661, 1618, 1567, 1507, 1440, 1389, 1365, 1335, 1240, 1160, 1111, 1071, 1045, 1013, 980, 892, 862, 806, 784, 770, 753, 730, 704, 677, 637 cm^{-1}. HRMS (ESI$^+$): *m/z* calcd for $C_{40}H_{39}N_3NaO_5$ $[M + Na]^+$ 664.2787, found 664.2782.

tert-Butyl(2-(2-(4-(2-(2-benzyl-1-phenylfuro[2,3-c]isoquinoline-5-carboxamido)ethyl)phenoxy) ethoxy)ethyl) carbamate **20**. The reaction between **17** (116 mg, 0.14 mmol), $PdCl_2(PPh_3)_2$ (4.8 mg, 6.87 μmol), phenylacetylene (30 μL, 0.27 mmol) and DBU (21 μL, 0.14 mmol) was carried out as described in the general procedure. The crude was eluted from a column of silica gel with PE/CH_2Cl_2/EtOAc (2:2:1) to give **20** (73 mg, 77%) as a yellow foam. R_f 0.42 (PE/CH_2Cl_2/EtOAc 2:2:1). ^{1}H NMR ($CDCl_3$, 300 MHz, δ ppm): 9.72 (d, J = 7.9 Hz, 1 H, CH Ar), 8.13 (broad t, J = 5.8 Hz, 1 H, NH), 7.77 (dd, J = 7.6, 1.6 Hz, 1 H, CH Ar), 7.61–7.46 (m, 7 H, 7 CH Ar), 7.34–7.17 (m, 7 H, 7 CH Ar), 6.92–6.83 (m, 2 H, 2 CH Ar), 4.99 (broad s, 1 H, NH), 4.13 (s, 2 H, CH_2), 4.10 (dd, J = 5.5, 3.9 Hz, 2 H, CH_2), 3.81 (dd, J = 5.4, 4.0 Hz, 2 H, CH_2), 3.74 (q, J = 6.8 Hz, 2 H, CH_2), 3.61 (t, J = 5.1 Hz, 2 H, CH_2), 3.34 (q, J = 5.2 Hz, 2 H, CH_2), 2.94 (t, J = 7.4 Hz, 2H, CH_2), 1.43 (s, 9 H, Boc). ^{13}C NMR (75 MHz, $CDCl_3$, δ ppm): 166.0 (C quat.), 157.3 (C quat.), 156.0 (C quat.), 154.4 (2 C quat.), 142.5 (C quat.), 137.2 (C quat.), 132.9 (C quat.), 132.3 (C quat.), 131.5 (C quat.), 130.3 (2 CH Ar), 130.0 (CH Ar), 129.8 (2 CH Ar), 129.0 (CH Ar), 128.97 (2 CH Ar), 128.7 (2 CH Ar), 128.6 (2 CH Ar), 128.4 (CH Ar), 126.8 (CH Ar), 126.3 (CH Ar), 125.1 (C quat.), 122.4 (CH Ar), 119.5 (C quat.), 116.3 (C quat.), 114.7 (2 CH Ar), 79.2 (C quat.), 70.4 (CH_2), 69.5 (CH_2), 67.3 (CH_2), 41.3 (CH_2), 40.3 (CH_2), 35.1 (CH_2), 32.8 (CH_2), 28.4 (Boc). HRMS (ESI$^+$): *m/z* calcd for $C_{42}H_{43}N_3NaO_6$ $[M + Na]^+$ 708.3050, found 708.3044.

2.1.6 General procedure for Boc removal (compounds **21**–**23**)

A solution of furo[2,3-*c*]isoquinoline (**18**, **19** or **20**, 30 mg) in CH_2Cl_2 (1 mL, 0.044–0.047 mol·L^{-1}) was treated at room temperature with trifluoroacetic acid (1 mL) for 2 h, until starting material was consumed (TLC monitoring, hexane/EtOAc 7:3). Then the solution was concentrated *in vacuo*. The crude was taken up with water and, after addition of saturated aqueous $NaHCO_3$ solution, an extraction with CH_2Cl_2 was performed. The combined

organic layers were dried ($MgSO_4$), and concentrated to give a colorless oil, pure enough for the following coupling.

N-(4-(3-aminopropoxy)phenethyl)-2-benzyl-1-phenylfuro[2,3-c]isoquinoline-5-carboxamide **21**. ^{1}H NMR ($CDCl_3$, 600 MHz, δ ppm): 9.53 (d, J = 8.5 Hz, 1 H, CH Ar), 8.21 (t, J = 5.7 Hz, 1 H, NH), 7.77 (d, J = 8.4 Hz, 1 H, CH Ar), 7.61–7.47 (m, 7 H, 7 CH Ar), 7.33–7.28 (m, 2 H, 2 CH Ar), 7.26–7.21 (m, 3 H, 3 CH Ar), 7.16 (d, J = 7.2 Hz, 2 H, 2 CH Ar), 6.80 (broad s, 2 H, 2 CH Ar), 4.11 (s, 2 H, CH_2), 4.05 (broad s, 2 H, CH_2), 3.76–3.63 (m, 2 H, CH_2), 3.26 (broad s, 2 H, NH_2), 2.91 (t, J = 7.1 Hz, 2 H, CH_2), 2.15 (broad s, 2 H, CH_2), 1.36–1.20 (m, 2 H, CH_2). ^{13}C NMR (150 MHz, $CDCl_3$, δ ppm): 166.7 (C quat.), 156.8 (C quat.), 154.9 (C quat.), 154.6 (C quat.), 142.5 (C quat.), 137.3 (C quat.), 133.2 (C quat.), 132.4 (C quat.), 132.2 (C quat.), 130.3 (2 CH Ar), 130.1 (CH Ar), 129.2 (2 CH Ar), 128.7 (3 CH Ar), 128.6 (3 CH Ar), 128.57 (CH Ar), 128.5 (CH Ar), 126.8 (CH Ar), 126.4 (CH Ar), 125.0 (C quat.), 122.8 (CH Ar), 119.8 (C quat.), 116.8 (C quat.), 114.9 (2 CH Ar), 66.5 (CH_2), 41.6 (CH_2), 35.2 (CH_2), 33.0 (CH_2), 29.9 (CH_2), 26.9 (CH_2). UV (DMSO, 10 μg·mL^{-1}, 18.0 μmol·L^{-1}): $\lambda_{max,abs}$ 353 nm, $\lambda_{max,em}$ 410 nm ($\lambda_{max,exc}$ 350 nm). HRMS (ESI$^+$): *m/z* calcd for $C_{36}H_{34}N_3O_3$ [M + H]$^+$ 556.2600, found 556.2595.

N-(4-(2-aminoethoxy)phenethyl)-2-benzyl-1-phenylfuro[2,3-c]isoquinoline-5-carboxamide **22**. ^{1}H NMR ($CDCl_3$, 600 MHz, δ ppm): 9.45 (d, J = 6.1 Hz, 1 H, CH Ar), 8.07 (broad s, 1 H, NH), 7.66 (d, J = 8.2 Hz, 1 H, CH Ar), 7.52–7.33 (m, 7 H, 7 CH Ar), 7.25–7.10 (m, 5 H, 5 CH Ar), 7.05 (broad s, 2 H, 2 CH Ar), 6.69 (broad s, 2 H, 2 CH Ar), 4.01 (broad s, 4 H, 2 CH_2), 3.56 (broad s, 2 H, CH_2), 3.20 (broad s, 2 H, NH_2), 2.78 (broad s, 2 H, CH_2), 1.23–1.14 (m, 2 H, CH_2). ^{13}C NMR (150 MHz, $CDCl_3$, δ ppm): 166.3 (C quat.), 156.2 (C quat.), 154.6 (C quat.), 154.4 (C quat.), 142.4 (C quat.), 137.2 (C quat.), 132.9 (C quat.), 132.4 (C quat.), 132.2 (C quat.), 130.3 (2 CH Ar), 130.1 (CH Ar), 129.9 (CH Ar), 129.0 (2 CH Ar), 128.7 (2 CH Ar), 128.67 (CH Ar), 128.6 (3 CH Ar), 128.4 (CH Ar), 126.8 (CH Ar), 126.4 (CH Ar), 125.0 (C quat.), 122.5 (CH Ar), 119.6 (C quat.), 116.4 (C quat.), 114.7 (2 CH Ar), 60.5 (CH_2), 41.2 (CH_2), 35.0 (CH_2), 32.7 (CH_2), 29.7 (CH_2). UV (DMSO, 10 μg·mL^{-1}, 18.4 μmol·L^{-1}): $\lambda_{max,abs}$ 354 nm, $\lambda_{max,em}$ 412 nm ($\lambda_{max,exc}$ 350 nm). HRMS (ESI$^+$): *m/z* calcd for $C_{35}H_{32}N_3O_3$ [M + H]$^+$ 542.2444, found 542.2438.

N-(4-(2-(2-aminoethoxy)ethoxy)phenethyl)-2-benzyl-1-phenylfuro[2,3-c]isoquinoline-5-carboxamide **23**. ^{1}H NMR ($CDCl_3$, 600 MHz, δ ppm): 9.52 (broad s, 1 H, CH Ar), 8.22 (broad s, 1 H, NH), 7.78 (d, J = 7.9 Hz, 1 H, CH Ar), 7.63–7.45 (m, 7 H, 7 CH), 7.34–7.11 (m, 7 H, 7 CH Ar), 6.84 (broad s, 2 H, 2 CH Ar), 4.20–4.10 (broad s, 4 H, 2 CH_2), 3.62 (broad s, 6 H, 3 CH_2), 3.18 (broad s, 2 H, NH_2), 2.92 (broad s, 2 H, 2 CH_2), 1.30 (broad s, 2 H, CH_2). ^{13}C NMR (150 MHz, $CDCl_3$, δ ppm): 166.6 (C quat.), 157.1 (C quat.), 154.6 (C quat.), 154.41 (C quat.), 142.6 (C quat.), 137.1 (C quat.), 133.0 (C quat.), 132.2 (C quat.), 131.9 (C quat.), 130.3 (2 CH Ar), 130.2 (CH Ar), 129.9 (CH Ar), 129.0 (CH Ar), 128.7 (2 CH Ar), 128.68 (CH Ar), 128.65 (2 CH Ar), 128.5 (CH Ar), 126.9 (CH Ar), 126.4 (2 CH Ar), 125.0 (C quat.), 122.6 (2 CH Ar), 119.6 (C quat.), 116.5 (C quat.), 115.0 (2 CH Ar), 70.1 (CH_2), 67.3 (CH_2), 41.3 (CH_2), 40.3 (CH_2), 34.7 (CH_2), 32.7 (CH_2), 28.9 (CH_2). UV (DMSO, 10 μg·mL^{-1}, 17.1 μmol·L^{-1}): $\lambda_{max,abs}$ 354 nm, $\lambda_{max,em}$ 412 nm ($\lambda_{max,exc}$ 350 nm). HRMS (ESI$^+$): *m/z* calcd for $C_{37}H_{36}N_3O_4$ [M + H]$^+$ 586.2706, found 586.2700.

2.2 Synthesis of CNOs, ligation to **21**–**23**, and characterization of the new nanomaterials

2.2.1 General

Thermogravimetric analyses (TGA) were conducted on a TA Q500 analyser, using a Pt pan as sample holder. After equilibrating the sample at 30°C for 5 min and then at 100°C for additional 20 min, the measurement was performed in air using a heating rate of 10°C·min^{-1}. The sample weight was monitored until 900°C. General remarks on UV-visible and fluorescence measurements are the same of the previous paragraph. The concentrations of the compounds under investigation were the same as those used for the UV-visible absorption measurements. DLS Measurements were performed on the Malvern Nano-ZS instrument operating in backscattering (173°) mode and analysed with the software Zetasizer, with automatic selection of the optimal detector position and number of independent measurements. For spectroscopic studies and DLS measurements, the CNOs were dispersed in DMSO to a final concentration of 500 μg·mL^{-1}. The dispersion of CNO was sonicated for 15 min at 37 kHz and then diluted respectively in DMSO to achieve final concentrations of 50, 20, 10, 5 and 1 μg·mL^{-1}. The CNOs samples were sonicated for additional 15 min and the size of the particle was measured.

2.2.2 Preparation of *p*-CNOs

The synthesis of small CNOs (6–8 shells) was performed by annealing nanodiamonds of 5 nm average particle size under a positive pressure of helium at 1650°C [47].

2.2.3 Preparation of *ox*-CNOs

Oxidation of *p*-CNOs was carried out following a procedure based on an earlier reported methodology [48]. A suspension of *p*-CNOs (100 mg) in a 3 mol·L^{-1} nitric acid solution (75 mL) was stirred at reflux for 48 h. After cooling to room temperature, the *ox*-CNOs were

filtered off through a nylon filter membrane (pore size 0.2 μm) and washed with water, methanol and acetone. The solid obtained was dried under high vacuum over night at room temperature. *ox*-CNOs (99 mg) were recovered as a black powder.

2.2.4 General procedure for ligation of **21**–**23** to CNOs

A dispersion of *ox*-CNO (10 mg for the synthesis of **1**-CNO and 15 mg for the synthesis of **2**- and **3**-CNO respectively) was ultrasonicated (20 min at 37 kHz) in a mixture of dry THF and *N*,*N*-dimethylformamide (DMF) (2:1, 30 mL). The mixture was deoxygenated under N_2 and 4-dimethylamino pyridine (DMAP, 20 mg, 163.7 μmol), *N*-hydroxysulfosuccinimide sodium salt (sulfo-NHS, 20 mg, 92.1 μmol) and *N*-ethyl-*N*′-(3-dimethylaminopropyl)carbodiimide hydrochloride (EDC, 35 mg, 182.6 μmol) were added. The reaction mixture was briefly sonicated and, after the addition of **21** (20 mg, 36.0 μmol), **22** (20 mg, 36.9 μmol) or **23** (20 mg, 34.1 μmol), it was heated under reflux for 4 d under N_2. After cooling to room temperature, the CNOs were re-dispersed in DMF, filtered off on a nylon membrane (pore size 0.2 μm) and washed with THF, DMSO and acetone in order to completely remove the furo[2,3-*c*]isoquinolines physically adsorbed on the surface of the CNOs. The resulting material was re-dispersed in DMSO, filtered again and centrifuged to wash out any non-covalently bound species.

2.2.5 **1**-CNO

The general procedure was followed and 12 mg of **1**-CNO were recovered as black powder after drying under air for one day. UV (DMSO, 10 $\mu g \cdot mL^{-1}$): $\lambda_{max,abs}$ 355 nm, $\lambda_{max,em}$ 400 nm ($\lambda_{max,exc}$ 350 nm).

2.2.6 **2**-CNO

The general procedure was followed and 14 mg of **2**-CNO were recovered as black powder after drying under air for one day. UV (DMSO, 10 $\mu g \cdot mL^{-1}$): $\lambda_{max,abs}$ 355 nm, $\lambda_{max,em}$ 408 nm ($\lambda_{max,exc}$ 350 nm).

2.2.7 **3**-CNO

The general procedure was followed and 12 mg of **3**-CNO were recovered as black powder after drying under air for one day. UV (DMSO, 10 $\mu g \cdot mL^{-1}$): $\lambda_{max,abs}$ 355 nm, $\lambda_{max,em}$ 398 nm ($\lambda_{max,exc}$ 350 nm).

3 Results and discussion

In recent years we published a very fast and efficient synthesis of an almost unknown heterocycle, the furo[2,3-*c*]isoquinoline scaffold **2** [49]. These molecules can be obtained through a highly convergent approach based on two key steps, as summarized in Scheme 1, where the most likely intermediates of the sequence are reported as well (the structure of **4** has been demonstrated). The synthesis starts with an Ugi multicomponent reaction (MCR) [50] in which an isocyanide, an aldehyde, a carboxylic acid and 2,4-dimethoxybenzyl amine are reacted together to afford peptide structure **1**. Apart from the well-known step and

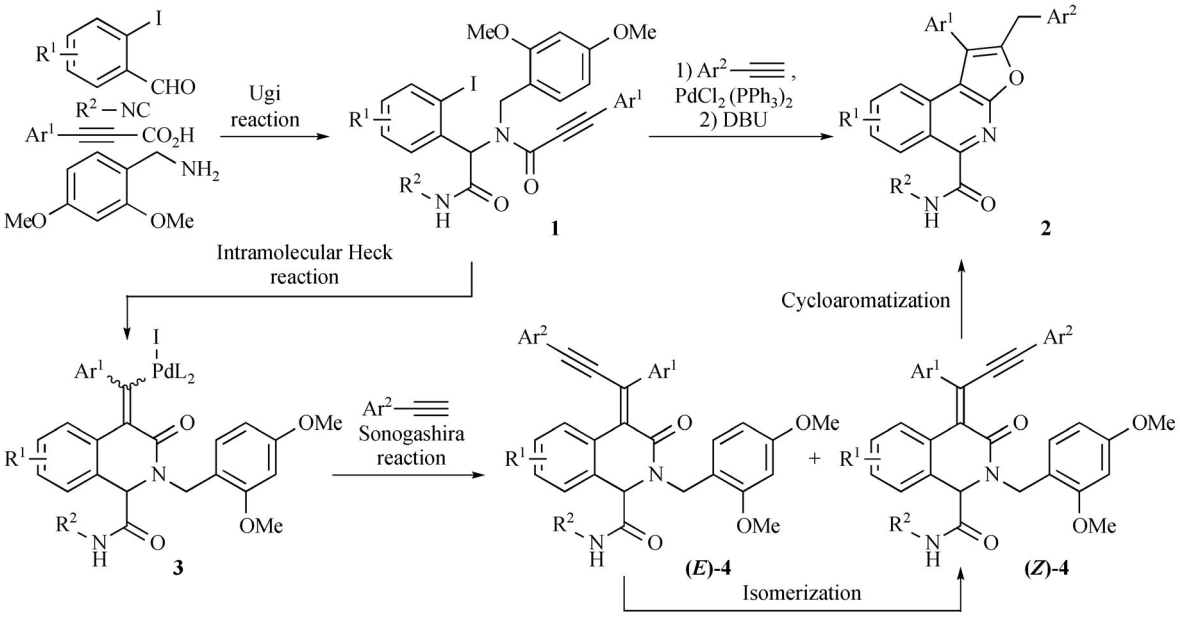

Scheme 1 Synthetic strategy to furo[2,3-*c*]isoquinolines **2**

atom economy, one of the main advantages of MCRs is that they allow a very efficient exploration of the chemical space, thanks to the possibility to fine tune the structure of the participating reagents. Actually, for the synthesis of scaffold **2** three features have to be respected: (a) The aldehyde must be necessarily aromatic with an iodine in the ortho position; (b) the carboxylic acid needs to be propiolic; (c) the amine can be only 2,4-dimethoxybenzyl amine because it is used as ammonia surrogate, which usually affords not well reproducible results in this MCR [49]. By contrast, the 2,4-dimethoxybenzyl group can be easily cleaved during the cyclization step. On the contrary, the decorations (i.e., R^1, R^2, Ar^1) can be varied at will, which is very important for tuning the properties (fluorescence, solubility etc.) of final compounds **2**.

Ugi products **1** are the substrates for a Pd-catalyzed insertion-alkynylation-cycloisomerization cascade in which a terminal alkyne (again Ar^2 can be varied) is incorporated. The sequence stemming for the formation of **2** can be explained as: (a) An intramolecular Heck reaction, affording Pd-intermediate **3**; (b) a Sonogashira coupling accounting for the formation of both (***Z***)- and (***E***)-**4** as the result of a poorly stereoselective Heck reaction; (c) a cycloaromatization in which the second cyclization occurs, while the spontaneous cleavage of the 2,4-dimethoxybenzyl group is promoted as well. Interestingly, if this step is performed in the presence of DBU the isomerization of the double bond of (***E***)-**4**, which is unable to cyclize for geometrical reasons, occurs, allowing therefore the transformation of both diastereoisomers of **4** into **2.**

All previously published compounds **2** are deep blue emitters with a λ_{em} in the range 400–425 nm, Stokes shifts up to 5600 cm^{-1} and a fluorescence quantum yield up to 0.90 with respect to 9,10-diphenylanthracene used as standard [49]. The photophysical properties are strictly dependent on the structure and electronic properties of the substituents, and of their position on the aromatic rings as well, as was clearly demonstrated with the synthesis of a second generation, not yet published, library of compounds **2**. Moreover, an appropriate modification of the

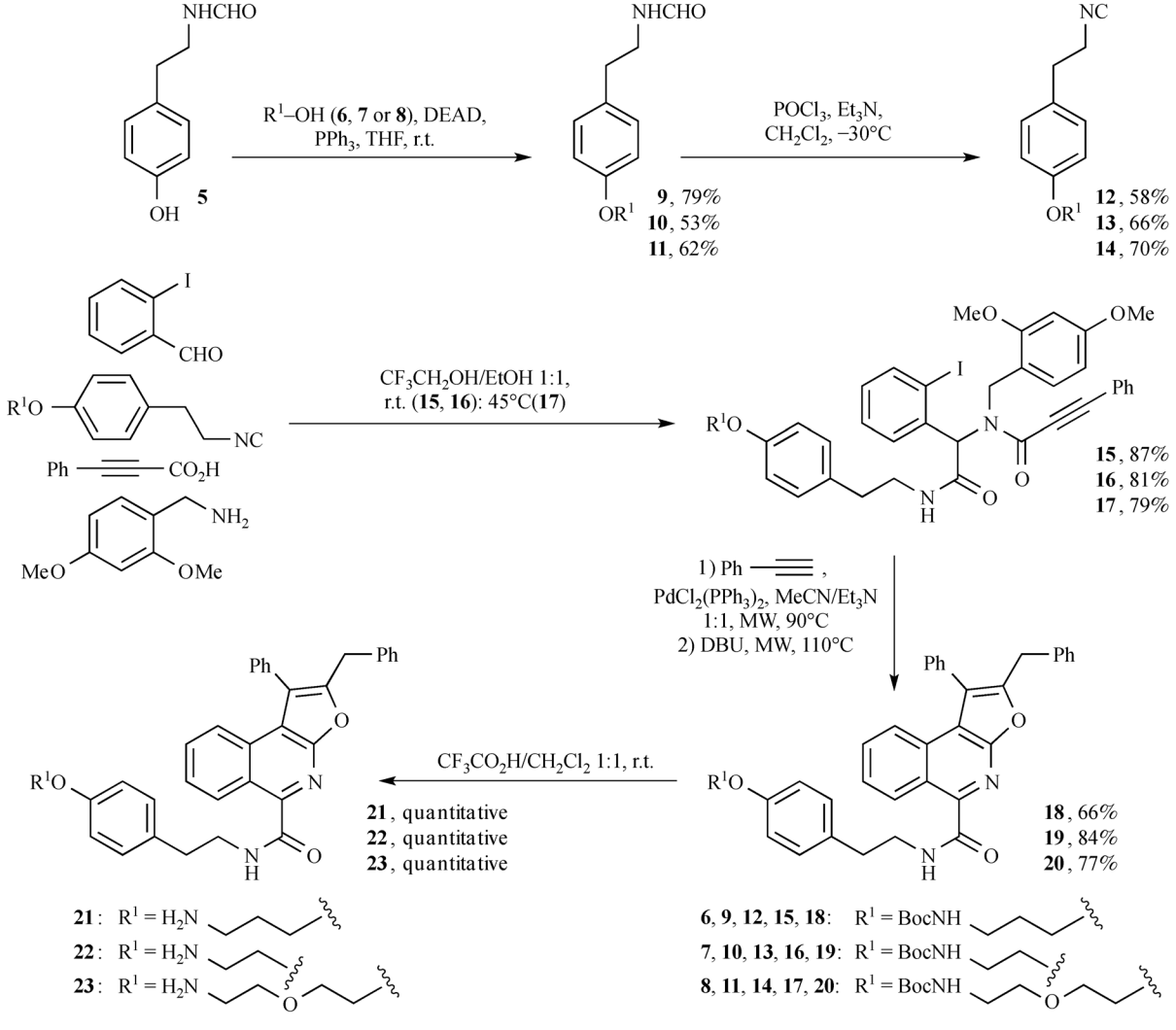

Scheme 2 Synthesis of furo[2,3-*c*]isoquinolines **21**–**23**

scaffold, still under investigation, has been demonstrated to be responsible for aggregation induced emission, which is very important for planning new fluorescent materials [51].

Since we wanted to obtain compounds with an additional functional group necessary for the conjugation to CNOs and, since the structure of the Ugi reagents can be varied at will, we initially decided to modulate group R^2, which is part of the isocyanide. The main reason is that this group does not significantly affect the photophysical properties of the molecule but, on the other hand, it can influence for example the solubility of the scaffold. In particular, we decided to synthesize three different isocyanides differing on the length and the structure of the chain separating the protected amino group and the common fragment bearing the isocyanide functionality, as summarized in Scheme 2.

As starting building block we used known formamide **5** [52] and we exploited the phenol group to introduce the desired Boc-protected amine through a Mitsunobu reaction, using commercially available Boc-amino alcohols **6** and **7**, or Boc-amino alcohol **8**, prepared as previously described [53]. Formamides **9**–**11** were then transformed into the corresponding isocyanides **12**–**14** under standard conditions requiring $POCl_3$ as dehydrating reagent, just before using them in the Ugi reaction. The isocyanides were combined with 2-iodobenzaldehyde, phenylpropiolic acid and 2,4-dimethoxybenzylamine to afford acyclic **15**–**17** in good overall yield. Then we applied the Pd-mediated cascade in order to transform them into furo[2,3-*c*] isoquinolines **18**–**20**. With our delight, the fluorophores were obtained in high yield (84%–66%), demonstrating the strength and versatility of our synthetic protocol. Finally, deprotection of the carbamate group under standard conditions (trifluoroacetic acid/CH_2Cl_2) afforded furo [2,3-*c*]isoquinolines **21**–**23**, characterized by a different spacer between the surface of the CNOs and the fluorescent heterocycles.

For the synthesis of *p*-CNOs we used the method developed by Kuznetsov [47], which results in gram quantities of nanoparticles with very high purity. The oxidation of the surface of the outer shell of *p*-CNOs was performed by refluxing them with nitric acid, which resulted in an extensive surface functionalization with carboxylic groups. With this method we realized a higher surface coverage compared to the Tour reaction yielding CNOs with higher reactivity [54]. Subsequently we developed a highly reproducible ligation methodology for the covalent modification of *ox*-CNOs with blue emissive compounds **21**–**23**. Actually, we exploited the formation of an amide bond between the free amino group of the fluorophores and the carboxylic acid groups on the

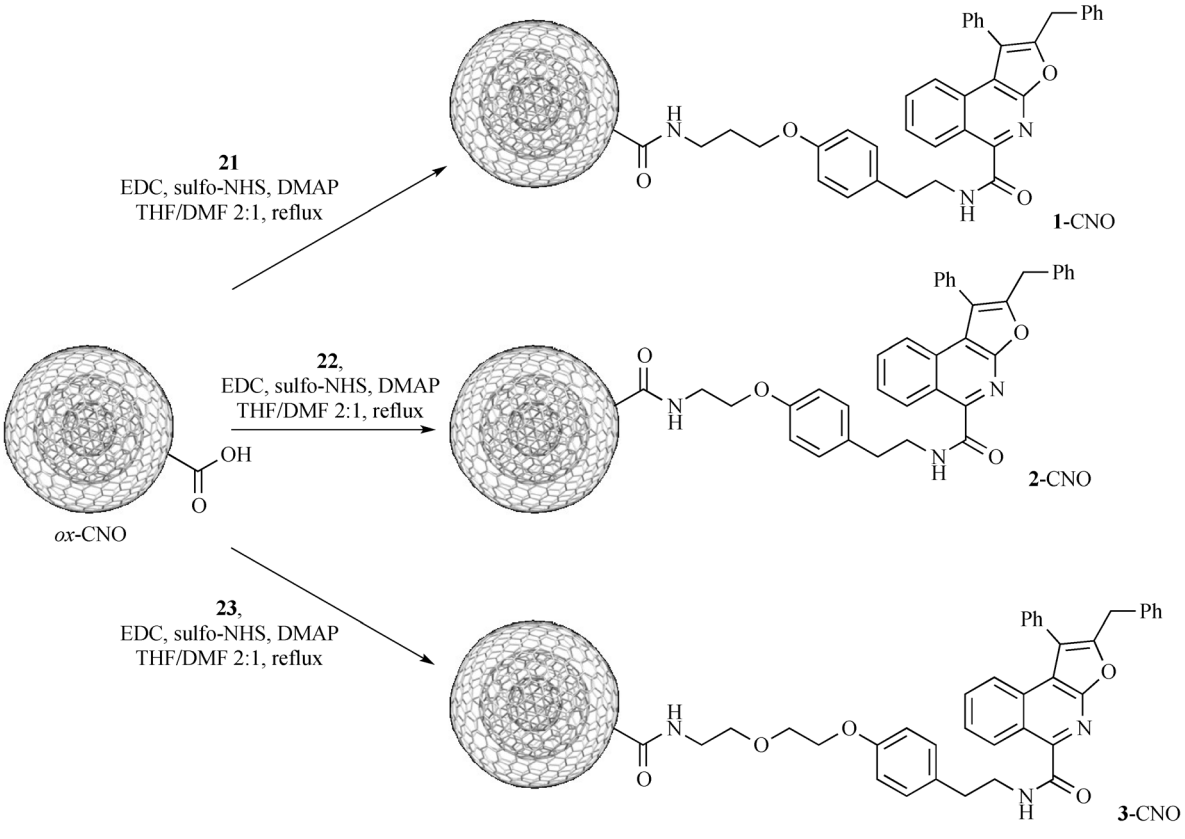

Scheme 3 Ligation of fluorophores **21**–**23** to *ox*-CNOs

surface of the CNOs, which was performed using EDC as coupling agent in the presence of sulfo-NHS and DMAP (Scheme 3).

The successful coupling of the *ox*-CNOs with **21**–**23** to obtain blue emissive **1**-CNO, **2**-CNO and **3**-CNO, was confirmed by TGA, absorption and emission spectroscopic studies, and dynamic light scattering (DLS) measurements. First of all, the high degree of surface functionalization of **1**-CNO, **2**-CNO and **3**-CNO (Fig. 1 on the top, red line) in comparison to the *ox*-CNO (blue line) was observed by TGA analysis. TGA, performed in air with a temperature rate of $10°C \cdot min^{-1}$, shows thermal decomposition of surface organics at 401°C, 380°C and 392°C for **1**-CNO, **2**-CNO and **3**-CNO respectively, followed by the decomposition of the CNO core at around 550°C. The average number of functional groups per onion has been estimated to be approx 60, 40 and 80 for **1**-CNO, **2**-CNO and **3**-CNO respectively, assuming that CNOs contain on average six shells and that the core is a C_{60} fullerene, as deducted by TEM observations.

The absorption and emission spectra of **1**-CNO, **2**-CNO and **3**-CNO (solid line) and the free furo[2,3-*c*]isoquinolines **21**, **22** and **23** (dotted line) in DMSO (c 10 $\mu g \cdot mL^{-1}$) are reported in Fig. 1 (middle and bottom sections respectively). Upon photoexcitation at 350 nm of dispersions of **1**-CNO, **2**-CNO and **3**-CNO (solid line) in DMSO, emission bands were observed with a maximum centered around 400 nm. The concentration of isoquinoline **21** in a 10 $\mu g \cdot mL^{-1}$ dispersion of **1**-CNO in DMSO was determined to be about 1.13×10^{-6} $mol \cdot L^{-1}$ by absorption. Similarly, concentrations of 4.65×10^{-5} $mol \cdot L^{-1}$ and 6.83×10^{-7} $mol \cdot L^{-1}$ were estimated for **2**-CNO and **3**-CNO respectively. The isoquinoline loadings were found to be comparable with the one we obtained conjugating green and red emitting dyes with CNOs [48,55]. Moreover, from the emission spectra, a quenching of approx 20% for **1**-CNO, 15% for **2**-CNO and 20% for **3**-CNO in comparison with the free blue emissive dyes **21**–**23** was observed, after excitation at the same wavelength. The reduced fluorescence intensity can be attributed to a high intrinsic absorption of the CNOs. Although, this fluorescence quenching is a drawback for imaging, it can be overcome by developing synthetic strategies to electronically separate the fluorophore from the nanomaterial.

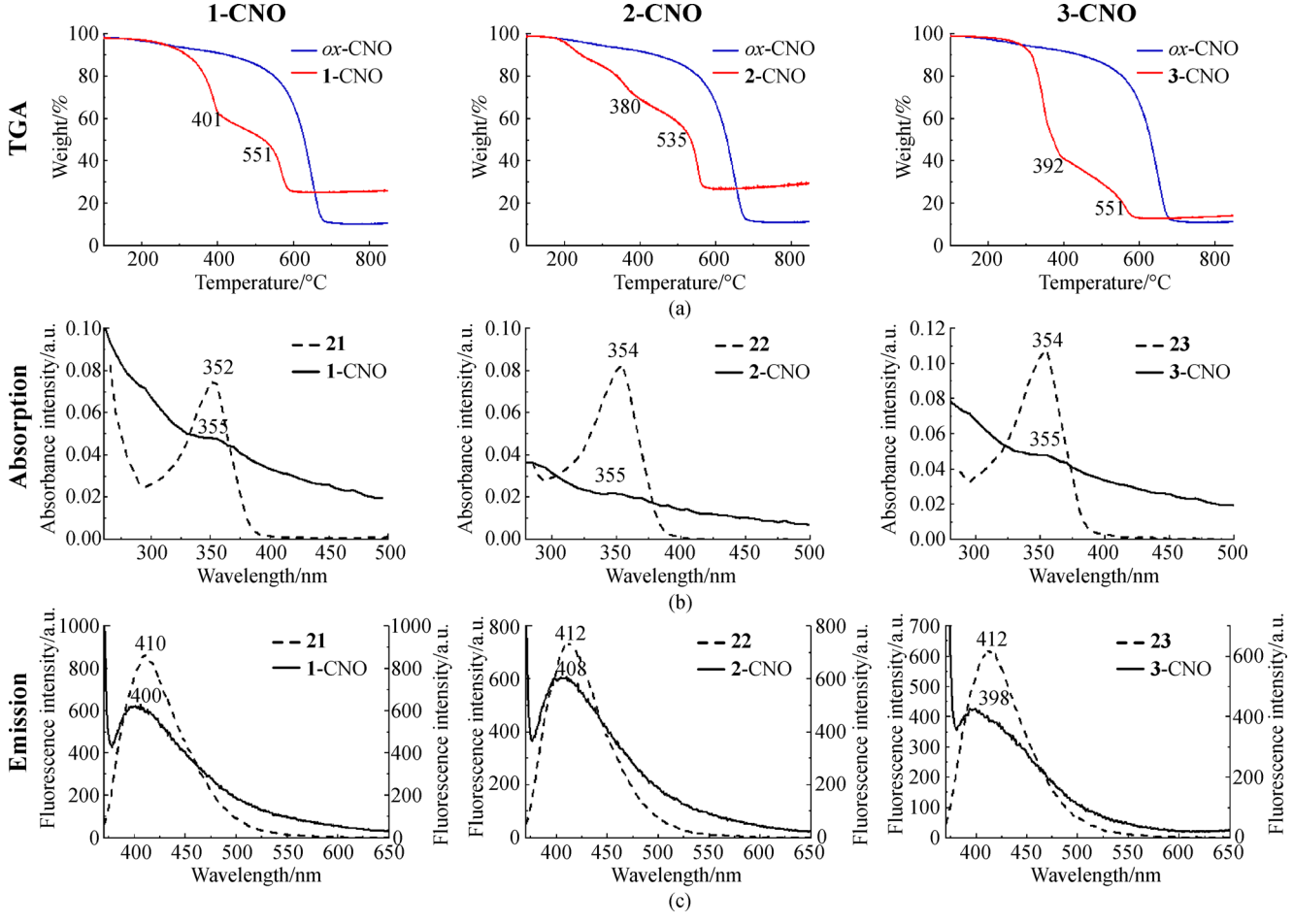

Fig. 1 (a) TGA analysis of CNOs before (*ox*-CNO) and after ligation (**1**-CNO, **2**-CNO, **3**-CNO), and (b) absorption and (c) emission spectra of fluorophores (**21**, **22** and **23**) before and after ligation.

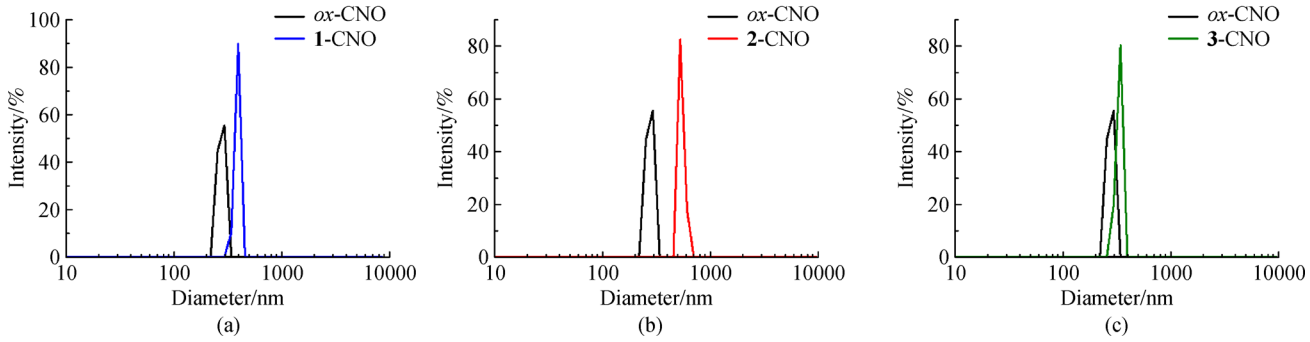

Fig. 2 Effective hydrodynamic diameter obtained from DLS measurements of **1**-CNO, **2**-CNO and **3**-CNO

This can be accomplished, for example, by the introduction of molecular spacers, biomolecules or coatings between the fluorophore and the CNO.

The size of the clusters formed were investigated by DLS in DMSO at a concentration of 10 $\mu g \cdot mL^{-1}$. DLS is driven by collisions with the solvent molecules present, which are in constant movement due to their thermal energy. According to that, this measurement depends on the size of the particle core, the surface structures, particle concentration, and the type of ions in the medium. After 20 min sonication *ox*-CNO revealed an effective hydrodynamic diameter of 277±1 nm. **1**-CNO, **2**-CNO and **3**-CNO revealed a hydrodynamic diameter of 390±1 nm, 546±5 nm and 332±2 nm respectively. The lowest value found was for **3**-CNO suggesting that the extra oxygen in the linker is favoring better dispersions (Fig. 2).

4 Conclusions

In summary, we have developed a versatile strategy for the preparation of deep blue emitting furo[2,3-c]isoquinolines, by coupling the multicomponent Ugi reaction with a complex Pd-mediated cascade and we showed their successful chemical functionalization on the surface of CNOs.

The high surface-to-volume ratio, chemical versatility and ease of manipulation of CNOs, as well as their performance as a chemically robust platform render these functionalized CNOs valuable candidate for blue high emissive materials.

The very versatile synthetic approach to our fluorophores opens the way also to differently functionalized scaffolds with this basic structure, simply modifying the building blocks to be used in the Ugi reaction. This would allow a fine tuning of the most important properties in the field of nanomaterials: The fluorescence and the solubility. Moreover, the fluorescence of these novel nanomaterials paves the way for the development of new architectures and studies in this field are still undergoing.

Acknowledgements Istituto Italiano di Tecnologia and the University of Genova are gratefully acknowledged for financial support. S.G. acknowledges the COST Action CA 15107 "Multi-Functional Nano-Carbon Composite Materials Network (MultiComp)". The authors wish to thank Prof. Luis Echegoyen (UTEP) for supervising V.M. in the synthesis of pristine CNOs.

References

1. Kroto H W, Heath J R, O'Brien S C, Curl R F, Smalley R E. C_{60}: Buckminsterfullerene. Nature, 1985, 318(6042): 162–163
2. Ugarte D. Curling and closure of graphitic networks under electron-beam irradiation. Nature, 1992, 359(6397): 707–709
3. Ugarte D. Onion-like graphitic particles. Carbon, 1995, 33(7): 989–993
4. Mykhailiv O, Zubyk H, Plonska-Brzezinska M E. Carbon nano-onions: Unique carbon nanostructures with fascinating properties and their potential applications. Inorganica Chimica Acta, 2017, 468: 49–66
5. Palkar A, Melin F, Cardona C M, Elliott B, Naskar A K, Edie D D, Kumbhar A, Echegoyen L. Reactivity differences between carbon nano onions (cnos) prepared by different methods. Chemistry, an Asian Journal, 2007, 2(5): 625–633
6. Kuznetsov V L, Zilberberg I L, Butenko Y V, Chuvilin A L, Segall B. Theoretical study of the formation of closed curved graphite-like structures during annealing of diamond surface. Journal of Applied Physics, 1999, 86(2): 863–870
7. Sano N, Wang H, Alexandrou I, Chhowalla M, Teo K B K, Amaratunga G A J, Iimura K. Properties of carbon onions produced by an arc discharge in water. Journal of Applied Physics, 2002, 92 (5): 2783–2788
8. Alexandrou I, Wang H, Sano N, Amaratunga G A J. Structure of carbon onions and nanotubes formed by arc in liquids. Journal of Chemical Physics, 2004, 120(2): 1055–1058
9. Dorobantu D, Bota P M, Boerasu I, Bojin D, Enachescu M. Pulse laser ablation system for carbon nano-onions fabrication. Surface Engineering and Applied Electrochemistry, 2014, 50(5): 390–394
10. Chen X H, Deng F M, Wang J X, Yang H S, Wu G T, Zhang X B, Peng J C, Li W Z. New method of carbon onion growth by radio-frequency plasma-enhanced chemical vapor deposition. Chemical

Physics Letters, 2001, 336(3): 201–204
11. Bartelmess J, Giordani S. Carbon nano-onions (multi-layer fullerenes): Chemistry and applications. Beilstein Journal of Nanotechnology, 2014, 5: 1980–1998
12. Georgakilas V, Guldi D M, Signorini R, Bozio R, Prato M. Organic functionalization and optical properties of carbon onions. Journal of the American Chemical Society, 2003, 125(47): 14268–14269
13. Liu Y, Vander Wal R L, Khabashesku V N. Functionalization of carbon nano-onions by direct fluorination. Chemistry of Materials, 2007, 19(4): 778–786
14. Rettenbacher A S, Perpall M W, Echegoyen L, Hudson J, Smith D W. Radical addition of a conjugated polymer to multilayer fullerenes (carbon nano-onions). Chemistry of Materials, 2007, 19 (6): 1411–1417
15. Cioffi C T, Palkar A, Melin F, Kumbhar A, Echegoyen L, Melle-Franco M, Zerbetto F, Rahman G M A, Ehli C, Sgobba V, Guldi D M, Prato M. A carbon nano-onion–ferrocene donor–acceptor system: Synthesis, characterization and properties. Chemistry (Weinheim an der Bergstrasse, Germany), 2009, 15(17): 4419–4427
16. Zhou L, Gao C, Zhu D, Xu W, Chen F F, Palkar A, Echegoyen L, Kong E S W. Facile functionalization of multilayer fullerenes (carbon nano-onions) by nitrene chemistry and "grafting from" strategy. Chemistry (Weinheim an der Bergstrasse, Germany), 2009, 15(6): 1389–1396
17. Flavin K, Chaur M N, Echegoyen L, Giordani S. Functionalization of multilayer fullerenes (carbon nano-onions) using diazonium compounds and "click" chemistry. Organic Letters, 2010, 12(4): 840–843
18. Tomita S, Fujii M, Hayashi S, Yamamoto K. Electron energy-loss spectroscopy of carbon onions. Chemical Physics Letters, 1999, 305 (3): 225–229
19. Chhowalla M, Wang H, Sano N, Teo K B K, Lee S B, Amaratunga G A J. Carbon onions: Carriers of the 217.5 nm interstellar absorption feature. Physical Review Letters, 2003, 90(15): 155504
20. Sek S, Breczko J, Plonska-Brzezinska M E, Wilczewska A Z, Echegoyen L. STM-based molecular junction of carbon nano-onion. ChemPhysChem, 2013, 14(1): 96–100
21. Zeiger M, Jäckel N, Aslan M, Weingarth D, Presser V. Understanding structure and porosity of nanodiamond-derived carbon onions. Carbon, 2015, 84: 584–598
22. Shenderova O, Tyler T, Cunningham G, Ray M, Walsh J, Casulli M, Hens S, McGuire G, Kuznetsov V, Lipa S. Nanodiamond and onion-like carbon polymer nanocomposites. Diamond and Related Materials, 2007, 16(4): 1213–1217
23. Macutkevic J, Adomavicius R, Krotkus A, Seliuta D, Valusis G, Maksimenko S, Kuzhir P, Batrakov K, Kuznetsov V, Moseenkov S, Shenderova O, Okotrub A V, Langlet R, Lambin P. Terahertz probing of onion-like carbon-PMMA composite films. Diamond and Related Materials, 2008, 17(7): 1608–1612
24. Bartolome J P, Echegoyen L, Fragoso A. Reactive carbon nano-onion modified glassy carbon surfaces as DNA sensors for human papillomavirus oncogene detection with enhanced sensitivity. Analytical Chemistry, 2015, 87(13): 6744–6751
25. Maffeis V, McCourt R O, Petracca R, Laethem O, Camisasca A, Colavita P E, Giordani S, Scanlan E M. Photocatalytic initiation of radical thiol-ene reactions using carbon-B_2O_3 nanocomposites. ACS Applied Nano Materials, 2018, 1(8): 4120–4126
26. Zeiger M, Jäckel N, Mochalin V N, Presser V. Review: Carbon onions for electrochemical energy storage. Journal of Materials Chemistry. A, Materials for Energy and Sustainability, 2016, 4(9): 3172–3196
27. Zheng D, Yang G, Zheng Y, Fan P, Ji R, Huang J, Zhang W, Yu J. Carbon nano-onions as a functional dopant to modify hole transporting layers for improving stability and performance of planar perovskite solar cells. Electrochimica Acta, 2017, 247: 548–557
28. D'Amora M, Rodio M, Bartelmess J, Sancataldo G, Brescia R, Cella Zanacchi F, Diaspro A, Giordani S. Biocompatibility and biodistribution of functionalized carbon nano-onions (f-CNOs) in a vertebrate model. Scientific Reports, 2016, 6(1): 33923
29. D'Amora M, Camisasca A, Lettieri S, Giordani S. Toxicity assessment of carbon nanomaterials in zebrafish during development. Nanomaterials (Basel, Switzerland), 2017, 7(12): 414
30. Trusel M, Baldrighi M, Marotta R, Gatto F, Pesce M, Frasconi M, Catelani T, Papaleo F, Pompa P P, Tonini R, Giordani S. Internalization of carbon nano-onions by hippocampal cells preserves neuronal circuit function and recognition memory. ACS Applied Materials & Interfaces, 2018, 10(20): 16952–16963
31. Lettieri S, d'Amora M, Camisasca A, Diaspro A, Giordani S. Carbon nano-onions as fluorescent on/off modulated nanoprobes for diagnostics. Beilstein Journal of Nanotechnology, 2017, 8: 1878–1888
32. Müller T J J, Bunz U H F. Functional Organic Materials. Syntheses, Strategies, and Applications. Weinheim: Wiley-VCH, 2007
33. Arcudi F, Đorđević L, Prato M. Rationally designed carbon nanodots towards pure white-light rmission. Angewandte Chemie International Edition, 2017, 56(15): 4170–4173
34. Frasconi M, Marotta R, Markey L, Flavin K, Spampinato V, Ceccone G, Echegoyen L, Scanlan E M, Giordani S. Multi-functionalized carbon nano-onions as imaging probes for cancer cells. Chemistry (Weinheim an der Bergstrasse, Germany), 2015, 21 (52): 19071–19080
35. Bartelmess J, Baldrighi M, Nardone V, Parisini E, Buck D, Echegoyen L, Giordani S. Synthesis and characterization of far-red/NIR-fluorescent BODIPY dyes, solid-state fluorescence, and application as fluorescent tags attached to carbon nano-onions. Chemistry (Weinheim an der Bergstrasse, Germany), 2015, 21(27): 9727–9732
36. Lettieri S, Camisasca A, d'Amora M, Diaspro A, Uchida T, Nakajima Y, Yanagisawa K, Maekawa T, Giordani S. Far-red fluorescent carbon nano-onions as a biocompatible platform for cellular imaging. RSC Advances, 2017, 7(72): 45676–45681
37. Liu Y, Kim D Y. Ultraviolet and blue emitting graphene quantum dots synthesized from carbon nano-onions and their comparison for metal ion sensing. Chemical Communications, 2015, 51(20): 4176–4179
38. Müllen K, Scherf U. Organic light-emitting diodes—synthesis, properties, and applications. Weinheim: Wiley-VCH, 2006
39. Zhu M, Yang C. Blue fluorescent emitters: Design tactics and applications in organic light-emitting diodes. Chemical Society Reviews, 2013, 42(12): 4963–4976
40. Kuma H, Hosokawa C. Blue fluorescent OLED materials and their

application for high-performance devices. Science and Technology of Advanced Materials, 2014, 15(3): 34201

41. Yang X, Xu X, Zhou G. Recent advances of the emitters for high performance deep-blue organic light-emitting diodes. Journal of Materials Chemistry. C, Materials for Optical and Electronic Devices, 2015, 3(5): 913–944
42. Bui T T, Goubard F, Ibrahim-Ouali M, Gigmes D, Dumur F. Thermally activated delayed fluorescence emitters for deep blue organic light emitting diodes: A review of recent advances. Applied Sciences (Basel, Switzerland), 2018, 8(4): 494
43. Froehlich J D, Young R, Nakamura T, Ohmori Y, Li S, Mochizuki A, Lauters M, Jabbour G E. Synthesis of Multi-Functional POSS Emitters for OLED Applications. Chemistry of Materials, 2007, 19 (20): 4991–4997
44. Krujatz F, Hild O R, Fehse K, Jahnel M, Werner A, Bley T. Exploiting the potential of oled-based photo-organic sensors for biotechnological applications. Chemical Sciences Journal, 2016, 7 (3): 134
45. Cairo C W, Key J A, Sadek C M. Fluorescent small-molecule probes of biochemistry at the plasma membrane. Current Opinion in Chemical Biology, 2010, 14(1): 57–63
46. Hong Y, Häußler M, Lam J W Y, Li Z, Sin K K, Dong Y, Tong H, Liu J, Qin A, Renneberg R, Tang B Z. Label-free fluorescent probing of G-quadruplex formation and real-time monitoring of dna folding by a quaternized tetraphenylethene salt with aggregation-induced emission characteristics. Chemistry (Weinheim an der Bergstrasse, Germany), 2008, 14(21): 6428–6437
47. Kuznetsov V L, Chuvilin A L, Butenko Y V, Mal'kov I Y, Titov V M. Onion-like carbon from ultra-disperse diamond. Chemical Physics Letters, 1994, 222(4): 343–348
48. Frasconi M, Maffeis V, Bartelmess J, Giordani S. Highly surface functionalized carbon nano-onions for bright light bioimaging. Methods and Applications in Fluorescence, 2015, 3(4): 0044005
49. Moni L, Gers-Panther C F, Anselmo M, Müller T J J, Riva R. Highly convergent synthesis of intensively blue emissive furo[2,3-*c*] isoquinolines by a palladium-catalyzed cyclization cascade of unsaturated Ugi products. Chemistry (Weinheim an der Bergstrasse, Germany), 2016, 22(6): 2020–2031
50. Dömling A. Recent developments in isocyanide based multi-component reactions in applied chemistry. Chemical Reviews, 2006, 106(1): 17–89
51. Hu R, Leung N L C, Tang B Z. AIE macromolecules: Syntheses, structures and functionalities. Chemical Society Reviews, 2014, 43 (13): 4494–4562
52. Banfi L, Basso A, Giardini L, Riva R, Rocca V, Guanti G. Tandem Ugi MCR/Mitsunobu cyclization as a short, protecting-group-free route to benzoxazinones with four diversity points. European Journal of Organic Chemistry, 2010, 2011(1): 100–109
53. Söveges B, Imre T, Póti Á L, Sok P, Kele Z, Alexa A, Kele P, Németh K. Tracking down protein–protein interactions via a FRET-system using site-specific thiol-labeling. Organic & Biomolecular Chemistry, 2018, 16(32): 5756–5763
54. Bartelmess J, De Luca E, Signorelli A, Baldrighi M, Becce M, Brescia R, Nardone V, Parisini E, Echegoyen L, Pompa P P, et al. Boron dipyrromethene (BODIPY) functionalized carbon nano-onions for high resolution cellular imaging. Nanoscale, 2014, 6(22): 13761–13769
55. Giordani S, Bartelmess J, Frasconi M, Biondi I, Cheung S, Grossi M, Wu D, Echegoyen L, O'Shea D F. NIR fluorescence labelled carbon nano-onions: Synthesis, analysis and cellular imaging. Journal of Materials Chemistry. B, Materials for Biology and Medicine, 2014, 2(42): 7459–7463